European Journal of Human Genetics (2015) 23, 766–773

www.nature.com/ejhg

ARTICLE

The expanding spectrum of *PRPS1*-associated phenotypes: three novel mutations segregating with X-linked hearing loss and mild peripheral neuropathy

Michela Robusto[1,7], Mingyan Fang[2,7], Rosanna Asselta[1], Pierangela Castorina[3], Stefano C Previtali[4], Sonia Caccia[1], Elena Benzoni[5], Raimondo De Cristofaro[6], Cong Yu[2], Antonio Cesarani[3], Xuanzhu Liu[2], Wangsheng Li[2], Paola Primignani[5], Umberto Ambrosetti[3], Xun Xu*[,2], Stefano Duga*[,1] and Giulia Soldà[1]

Next-generation sequencing is currently the technology of choice for gene/mutation discovery in genetically-heterogeneous disorders, such as inherited sensorineural hearing loss (HL). Whole-exome sequencing of a single Italian proband affected by non-syndromic HL identified a novel missense variant within the *PRPS1* gene (NM_002764.3:c.337G>T (p.A113S)) segregating with post-lingual, bilateral, progressive deafness in the proband's family. Defects in this gene, encoding the phosphoribosyl pyrophosphate synthetase 1 (PRS-I) enzyme, determine either X-linked syndromic conditions associated with hearing impairment (eg, Arts syndrome and Charcot-Marie-Tooth neuropathy type X-5) or non-syndromic HL (*DFNX1*). A subsequent screening of the entire *PRPS1* gene in 16 unrelated probands from X-linked deaf families led to the discovery of two additional missense variants (c.343A>G (p.M115V) and c.925G>T (p.V309F)) segregating with hearing impairment, and associated with mildly-symptomatic peripheral neuropathy. All three variants result in a marked reduction (>60%) of the PRS-I activity in the patients' erythrocytes, with c.343A>G (p.M115V) and c.925G>T (p.V309F) affecting more severely the enzyme function. Our data significantly expand the current spectrum of pathogenic variants in *PRPS1,* confirming that they are associated with a continuum disease spectrum, thus stressing the importance of functional studies and detailed clinical investigations for genotype–phenotype correlation.
European Journal of Human Genetics (2015) **23,** 766–773; doi:10.1038/ejhg.2014.168; published online 3 September 2014

INTRODUCTION

Hearing loss (HL) is the most common disabling disorder in humans, affecting about 360 million people worldwide (http://www.who.int/mediacentre/factsheets/fs300/en/index.html). It is estimated that about 60–70% of cases are due to genetic factors[1] of which about 5% are transmitted as X-linked traits. Overall, inherited HL is characterized by a high genetic heterogeneity, with >70 causal genes identified so far (http://www.hereditaryhearingloss.org), and many still to be discovered.

The extremely high number of HL-causing genes, as well as the low frequency of most known mutations, leave the majority of patients with no definitive genetic diagnosis, principally because the screening of all known deafness genes by traditional mutation analysis methods is unfeasible. Instead, whole-exome sequencing (WES) currently represents one of the most efficient strategy to search for rare variants underlying Mendelian diseases, and has already been applied to the discovery of novel genes/mutations responsible for autosomal (*DFNB82*) and X-linked (*DFNX4*) recessive non-syndromic sensorineural hearing loss (NSHL).[2–4] Before the identification of *SMPX* as the causative gene at the *DFNX4 locus*, only two other genes, *POU3F4* (*DFNX2*, OMIM #304400) and *PRPS1* (*DFNX1*, OMIM #304500), were clearly associated with X-linked forms of deafness.[5,6]

PRPS1 codes for phosphoribosyl pyrophosphate synthetase 1 (PRS-I), which catalyzes the synthesis of phosphoribosyl pyrophosphate (PRPP) from ATP and ribose-5-phosphate, and is essential for the *de-novo* synthesis of nucleotides in both eukaryotes and prokaryotes.[7]

The *DFNX1 locus* is associated with phenotypically heterogeneous NSHL. In general, hearing impairment in male patients with *PRPS1* mutations is bilateral, moderate to profound, and can be pre- or post-lingual, progressive or non-progressive. Female carriers may also be affected by unilateral or bilateral hearing impairment. So far, five *DFNX1* families were described, four with post-lingual progressive NSHL, and one with congenital profound deafness.[6] Four missense variants in *PRPS1* (NM_002764.3: c.193G>A (p.D65N), c.259G>A (p.A87T), c.869T>C (p.I290T), and c.916G>A (p.G306R) were identified in these families as disease causing. All of them result in a reduction of about half of PRS-I activity, as shown by *in-vitro* enzymatic assays on patients' erythrocytes and cultured fibroblasts. None of these mutations are predicted to cause a major structural change in the PRS-I protein.[6,8]

[1]Dipartimento di Biotecnologie Mediche e Medicina Traslazionale, Università degli Studi di Milano, Milan, Italy; [2]BGI-Shenzhen, Shenzhen, China; [3]Dipartimento di Scienze Cliniche e di Comunità, Università degli Studi di Milano, Fondazione IRCCS Cà Granda Ospedale Maggiore Policlinico, UO Audiologia, Milan, Italy; [4]Division of Neuroscience, Institute of Experimental Neurology, San Raffaele Scientific Institute, Milan, Italy; [5]Laboratory of Medical Genetics, Molecular Genetic Sector, Fondazione IRCCS Cà Granda Ospedale Maggiore Policlinico, Milan, Italy; [6]Haemostasis Research Center, Institute of Internal Medicine and Geriatrics, Catholic University School of Medicine, Rome, Italy
*Correspondence: Dr X Xu, BGI-Shenzhen, Shenzhen, China. Tel: +86 18688745853, Fax: +86 755 25273620; E-mail: xuxun@genomics.cn
or Professor S Duga, Dipartimento di Biotecnologie Mediche e Medicina Traslazionale, Università degli Studi di Milano, Via Viotti 3/5, 20133 Milan, Italy. Tel: +39 250315823; Fax: +39 250315864; E-mail: stefano.duga@unimi.it
[7]Shared first authorship.
Received 7 March 2014; revised 30 May 2014; accepted 5 June 2014; published online 3 September 2014

Mutations in *PRPS1* might also result in a spectrum of syndromic conditions, including PRS-I superactivity (OMIM #300661; eight mutations so far identified),[9,10] Charcot-Marie Tooth neuropathy type X-5 (CMTX5 or Rosenberg-Chutorian syndrome, OMIM #311070; three known mutations),[11,12] and Arts syndrome (OMIM #301835; three mutations reported to date).[13,14] In general, *PRPS1* gain-of-function mutations determine a loss of feedback regulation and hence enzyme superactivity, which in turn causes excessive uric acid production and gout. Conversely, loss-of-function mutations are responsible for NSHL, CMTX5, or Arts syndrome. In this case, the severity of the phenotype seems to correlate with the residual functionality of the enzyme, with milder mutations resulting only in HL, and more severe genetic defects causing also peripheral neuropathy (CMTX5), or central nervous system involvement and increased liability to infections (Arts syndrome). Taken together, these findings suggest that the four *PRPS1*-related phenotypes are part of the same disease spectrum,[10,14,15] thus stressing the importance of the functional characterization of pathogenic variants as well as the interpretation of genotype/phenotype correlations. In particular, CMTX5, which is characterized by a triad of symptoms: early-onset bilateral profound HL, peripheral neuropathy, and optic neuropathy, might be under-recognized by physicians and thus under-diagnosed.[15]

Here, we used a WES approach to search for novel genetic determinants of NSHL in a genetically-undiagnosed Italian family, leading to the identification of a novel missense variant in *PRPS1*. Two additional novel variants in *PRPS1* were discovered by extending the screening of the gene to 16 X-linked HL families. *PRPS1* variants were functionally characterized to assess their impact on the enzyme activity, and detailed neurological evaluation was performed to refine genotype/phenotype correlations.

MATERIALS AND METHODS

Patients

This study was approved by local Ethical Committees and performed according to the Declaration of Helsinki and to the Italian legislation on sensible data recording. Signed informed consent was obtained from all participants and from parents of subjects younger than 18 years.

Genomic DNA extraction from peripheral blood was performed using a semi-automatic DNA extractor (Fujifilm Europe GmBH, Düsseldorf, Germany), whereas DNA from buccal swabs from young children was purified according to the QIAamp DNA Mini Kit extraction protocol (Qiagen, Hilden, Germany). DNA samples were quantified on a Nanodrop ND-1000 spectrophotometer (NanoDrop Technologies, Wilmington, DE, USA), and stored at -20°C. All recruited patients did not carry mutations within gap-junction proteins connexin 26 and 30 (*GJB2*, *GJB6*), and the mitochondrial 12S rRNA (*MTRNR1*) genes. Genetic screening of *GJB2*, *GJB6*, and *MTRNR1* was performed as described.[16]

Audiological evaluation

A total of 17 genetically-undiagnosed NSHL families with a likely X-linked inheritance pattern were recruited from the Genetic Service and the Audiology Unit of the Ospedale Maggiore Policlinico of Milan. Clinical history ruled out environmental factors as cause of the HL and physical examination did not reveal any evidence of dysmorphic features.

All patients underwent ear, nose, and throat, and audiological examinations. For adults and collaborative children, hearing levels were determined by pure-tone audiometry, in accordance with International Standard Organization (ISI 8253-1-3) protocols. The hearing impairment diagnosis of young children (<1 year) was obtained through the auditory brainstem responses and the observation of their behaviors, whereas in older children a behavioral audiometry was performed. In addition, evoked otoacoustic emissions and tympanometry with acoustic reflex thresholds were evaluated. Average thresholds in the range of 21–40 dB were defined as mild, 41–70 dB as moderate, 71–95 dB as severe, and >95 dB as profound HL.

A total of 123 individuals with no familial history of HL and instrumentally-verified normal auditory function (mean age at withdrawal 32 ± 9) were also collected as controls.

Neurological evaluation

Patients underwent a standard neurological examination, including evaluation of muscle weakness and disability, gait, sensory loss, deep tendon reflexes, coordination, the presence of pyramidal or cerebellar signs, cranial nerve involvement, as well as the presence of bone abnormalities, joint retractions, and skin lesions.

Patients were evaluated with electromyography (EMG) and motor and sensory electroneurography, and routine laboratory tests including muscle enzymes, transaminases, metabolites, electrolytes, and screening for disimmune/inflammatory disorders.

Exome sequencing

One NSHL family (Family 1), with a recessive inheritance pattern and two affected individuals (Figure 1a), was selected for WES. Genomic capture and sequencing were performed on a single proband (II-2), using 3 μg of genomic DNA and the SureSelect 38M human exome kit (Agilent, Santa Clara, CA, USA). WES yielded 4.8 Gb raw sequence data with about 97.5% coverage of the targeted exome with a mean coverage of $\geq 50\times$ (Supplementary Methods and Supplementary Figure 1). Sequences were aligned to the human reference genome (hg18, NCBI build 36.3) using SOAPaligner/SOAP2 v.2.21[17] and genotypes were determined by the SOAPsnp software v.1.03 (Supplementary Methods). The called variants were annotated according to their position and predicted functional impact on the protein (Supplementary Methods and Supplementary Tables 1 and 2). Rare and potentially deleterious variants mapping within known NSHL *loci* were extracted and prioritized for validation. Sanger sequencing was used to confirm the presence of the identified potential disease-causing variants and to verify their segregation with the phenotype within Family 1.

PRPS1 mutational screening

All exons and exon-intron boundaries of *PRPS1* were PCR amplified using sets of primers designed on the basis of the known genomic sequence of the gene (GenBank accession number NG_008407.1). PCRs were performed on 10–20 ng of genomic DNA, following standard procedures. Primer sequences, as well as the specific PCR conditions for each primer couple are available on request.

Direct sequencing of amplified fragments was performed on both strands by means of the BigDye Terminator Cycle Sequencing Ready Reaction Kit v.1.1 and an automated ABI-3130XL DNA sequencer (Applied Biosystem, Foster City, CA, USA). The Variant Reporter software (Applied Biosystems) was used for variant detection.

Clinically-relevant variants and probands' phenotypes were deposited in the LOVD X-chromosome gene database (http://grenada.lumc.nl/LOVD2/MR/home.php?select_db=PRPS1) and to the ClinVar database (http://www.ncbi.nlm.nih.gov/clinvar/).

Molecular modeling

The effects of the c.337G>T (p.A113S), c.343A>G (p.M115V), and c.925G>T (p.V309F) variants on the structure of PRS-I were examined using the coordinates of the 3D-model of the homohexamer kindly provided by Dr SB Nabuurs and Dr A de Brouwer,[13] as well as the coordinates of the crystal structure of the human protein (PDB entry 2H06; http://www.pdb.org).[18] The analysis was performed using the FoldX plugin for the Yet Another Scientific Artificial Reality Application (YASARA) program.[19–21] This algorithm allowed us to evaluate the effect of variants on the stability of a single subunit and on the interaction energy of the subunits in the complex. Figures were produced using PyMOL (DeLano Scientific, San Carlos, CA, USA; http://www.pymol.org).

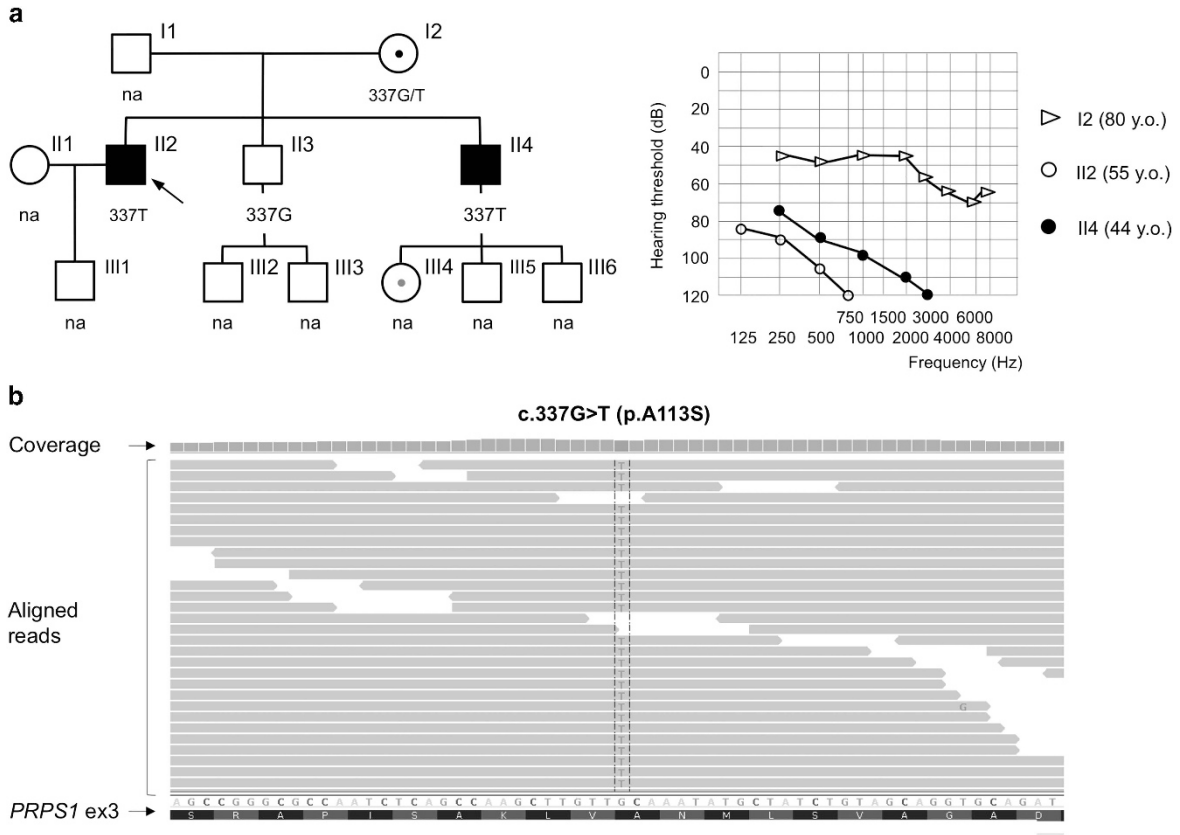

Figure 1 Identification of the novel *PRPS1* variant c.337G>T (p.A113S) segregating with NSHL by whole-exome sequencing. (**a**) Pedigree of Family 1 and audiograms of both affected males and one carrier female (average HL for the right and left ears is shown). This family, which showed a clear recessive inheritance pattern of the disease, was selected for targeted capture and exome sequencing (the analyzed subject is pointed by an arrow). The genotype of each individual is indicated below the corresponding symbols. na: not analyzed. (**b**) IGV (Integrative Genome Viewer) screenshot showing sequencing reads that support the mutant allele (the T nucleotide is reported) identified in the II2 proband. The identified G>T transversion maps within *PRPS1* exon 3 and results in the A113S amino-acid change. The mean coverage of the region here shown is 31.

PRS-I activity assay

Venous blood samples were collected in EDTA tubes from five wild-type subjects (one healthy sibling of an affected patient and four unrelated controls), five affected males, as well as four female carriers of *PRPS1* missense variants.

Immediately after phlebotomy, peripheral blood mononuclear cells (PBMCs) and erythrocytes were separated on a Lympholyte Cell separation media (Cederlane Laboratories Limited, Hornby, Ontario, Canada) gradient. Red cells were washed three times in phosphate-buffered saline, packed, and stored at −20°C. On the day of the assay, each sample was thawed and treated with activated charcoal (3 mg/ml) for 15 min at 4°C. After centrifugation, the supernatant was assayed for PRS-I activity, as described.[22] Briefly, the hemolysates were incubated for 60 min at 37°C with saturating amounts of substrates and an inhibitor of adenylate kinase (Ap5A) to prevent conversion of AMP into ADP. Aliquots of each reaction were terminated at five different times, and proteins removed by filtration. Control reactions without ribose-5-phosphate were set up using the hemolysate of a healthy control. ATP, ADP, and AMP in the filtrate were separated and quantitated by high-performance liquid chromatography (HPLC).

The hemoglobin content for each hemolysate was determined by the Drabkin method,[23] and used for normalization.

HPLC separation

Samples were appropriately diluted and injected into an HPLC C_{18} column (ReproSil-Pur C18-AQ RP-HPLC; Dr Maisch GmbH, Ammerbuch-Entringen, Germany) and eluted at room temperature with 50 mM $K(Na)H_2PO_4$ (pH 6.0) at a flow rate of 1.0 ml/min, as described.[22] The HPLC apparatus was a double-pump Model 2080 HPLC system equipped with a Model 2070 UV spectrophotometric and a FP-2020 fluorescence detector (Jasco, Tokyo, Japan). Absorbance was measured at 254 nm, and different concentrations of AMP and ATP (100–3.25 μM) were injected as standard. PRS-I activity was expressed as concentration of AMP generated per time unit and per mg of hemoglobin in the hemolysate.

RESULTS

Exome sequencing identifies a novel *PRPS1* missense variant segregating with NSHL

We sequenced the exome of one individual (II2) from an Italian family (Family 1) affected by post-lingual bilateral profound NSHL, with a likely recessive pattern of inheritance (autosomal or X-linked). The patient is a profoundly deaf 55-year-old man with a severely affected brother, one normal-hearing brother and one normal-hearing child (Figure 1a); both the patient and his brother had normal speech development, and received bilateral cochlear implants. The proband's mother (80 years old) has developed a late-onset moderate HL.

Approximately 2 Gb of polished sequence data mapping to the exome-targeted region was generated as paired-end, 90-bp reads. Nearly 97% of the intended target was covered with an average depth of 58×, with >80% of target covered >10× (Supplementary Figure 1). To identify potentially pathogenic mutations among called variants, we focused on rare (eg, not annotated in dbSNP130, 1000 Genome project, or Exome Variant Server, ESV) non-synonymous

(NS) variants, splice-site (SS) variants, and short coding insertions or deletions (indels; I). Under a recessive model, we then looked for homozygous/hemizygous or compound heterozygous variations, and prioritized those variants located in known deafness genes (Supplementary Table 3). This analysis revealed as the most promising candidate a novel missense variant within exon 3 of *PRPS1*, a gene already known to be associated with X-linked syndromic and non-syndromic HL.[8] The variant was a NM_002764.3:c.337G>T transversion, which results in the substitution of the Alanine at position 113 with a Serine (NP_002755.1:p.A113S). This variant segregates with the NSHL phenotype in the patient's family, being present in the hemizygous state in both affected males (II2 and II4) and in the heterozygous state in the I2 obligate female carrier (Figure 1). The variant was absent in a cohort of 123 Italian normal-hearing controls.

PRPS1 mutations are a frequent cause of X-linked deafness

To determine the incidence of *PRPS1* mutations in X-linked sensorineural deafness, we screened by Sanger sequencing all seven *PRPS1* exons, including intron-exon boundaries, in 16 additional unrelated male patients with familial history of HL, without reported neurological symptoms, and a likely X-linked inheritance pattern.

Among these, we identified two additional novel missense variants. One was a NM_002764.3:c.343A>G transition in *PRPS1* exon 3, leading to the NP_002755.1:p.M115V amino-acid change, which was found in a 12-year-old Italian patient affected by post-lingual progressive bilateral hearing impairment. The proband has a normal-hearing brother, two affected cousins and two affected uncles (Figure 2a). He presents a down-sloping audiometric profile, with moderate HL at low and middle frequencies and a severe hearing impairment at higher frequencies. The proband's mother suffers from a mild form of deafness. The variant segregates with HL in Family 2 (Figure 2a).

Finally, the third identified variant was a NM_002764.3:c.925G>T transversion in *PRPS1* exon 7, which results in the substitution of the Valine at position 309 with a Phenylalanine (NP_002755.1:p.V309F). This variant was found in a 14-year-old proband from a Peruvian family (Family 3) affected by post-lingual bilateral progressive deafness, characterized by a audiometric profile very similar to that of the Family 2 proband. The variant segregates with X-linked HL in the family (Figure 2b). Both identified variants were not annotated in general SNP databases (ie, dbSNP, 1000 Genome Project, ESV).

The p.(M115V) and p.(V309F) variants are associated with unrecognized peripheral neuropathy

As *PRPS1* mutations may cause peripheral neuropathy, all patients carrying *PRPS1* missense variants underwent neurological evaluation at the Clinical Centre for hereditary neuropathies (Ospedale San Raffaele, Milano). Among the three families, patients in Family 2 (c.343A>G (p.M115V)) and Family 3 (c.925G>T (p.V309F)) showed clinical or subclinical signs of peripheral neuropathy (Supplementary Table 4). As expected, males and females showed significant differences at neurological examination: in females we only observed subclinical signs of peripheral neuropathy (pes cavus, reduced or absent deep tendon reflexes, chronic denervation in distal muscles of lower limbs), whereas males displayed more evident findings of neuropathy. Even in males, the neuropathy was mildly symptomatic, did not cause weakness or evident motor deficits (except for III2, Family 2), whereas prevailed sensory signs and symptoms, such as Romberg positivity, absent deep tendon reflexes,

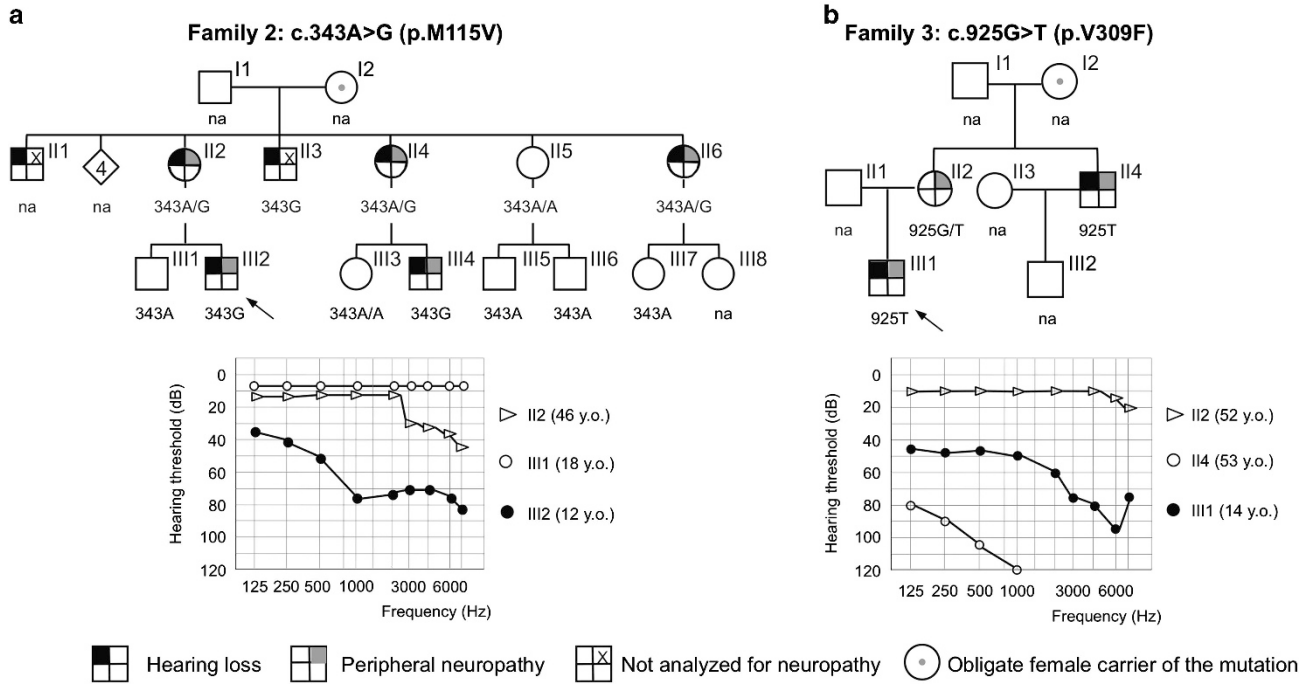

Figure 2 Identification of novel missense variants (c.343A>G (p.M115V) and c.925G>T (p.V309F)) in *PRPS1* in two additional families with X-linked deafness. Pedigree of Families 2 (**a**) and 3 (**b**) and the corresponding audiograms, showing the average HL for the right and left ears. The genotype of each individual is indicated below the corresponding symbol. Audiological and neurological phenotypes are indicated separately using different shades of gray. All female carriers had significantly milder phenotypes compared with affected males of the same family. The probands are pointed by an arrow. na: not analyzed.

paresthesias, and cramps. Almost all patients, except the carrier female from family 3, showed chronic denervation at EMG evaluation, whereas only males showed mild/moderate axonal neuropathy. In Family 2, we observed reduction of both motor and sensory nerve amplitudes, whereas in Family 3 only motor nerves were affected.

The newly identified *PRPS1* missense variants significantly reduce the enzyme activity *in vivo*

To assess the consequences of newly identified variants on protein function, we measured PRS-I enzymatic activity in erythrocytes from five affected males (II2 and II4 from Family 1, carrying the p.(A113S) substitution; III2 and III4 from Family 2 carrying the p.(M115V) variant; and III1 from Family 3, carrying the p.(V309F) change), four female carriers, three with the p.(M115V) substitution (II2, II4, and II6 from Family 2) and one with the p.(V309F) variant (II2, Family 3), as well as one unaffected male (III1 from Family 2) and four unrelated healthy controls (CTR1-4; two males, two females). The assay is based on HPLC measurement of AMP, which is produced in equimolar amounts with PRPP (see Materials and Methods for details).

Statistically significant differences in PRS-I activity in erythrocytes of affected males, female carriers, and wild-type controls were observed (ANOVA $P<2\times10^{-5}$, at time point 60 min) (Figure 3). In particular, a significant reduction was evident in affected males, although the impairment in the enzymatic activity seemed less severe in patients carrying the p.(A113S) variant than in the probands with the p.(M115V) or p.(V309F) substitutions. Indeed, PRS-I activity in

a

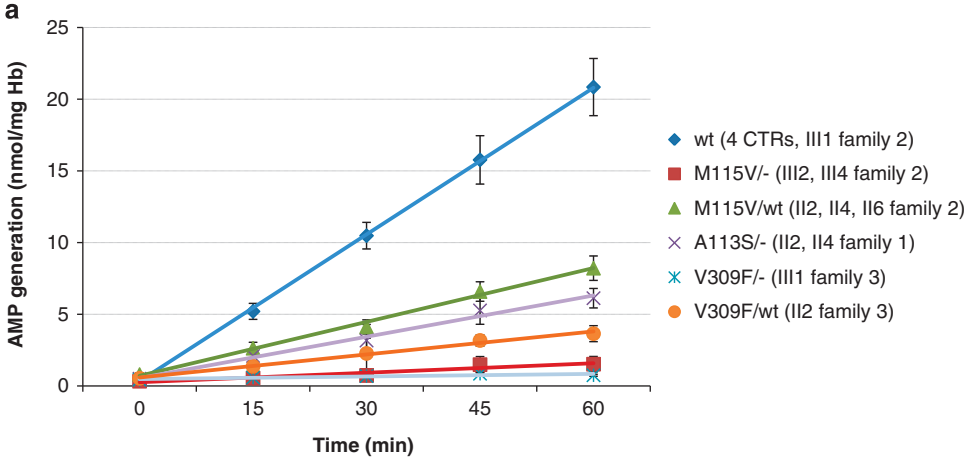

b

PRS-I Activity Assay in Erythrocytes from Family 1, 2, and 3

Individual	*Sex*	*Genotype*	*Age at testing*	*Activity (±SD) (nmol/mg/hr)*	*Percentage*
Affected Males					
II2 family 1	M	A113S/-	54	5.29 (±1.38)	25.4
II4 family 1	M	A113S/-	43	7.33 (±0.37)	35.2
III2 family 2	M	M115V/-	12	2.11 (±1.32)	10.2
III4 family 2	M	M115V/-	9	1.06 (±0.19)	5.1
II1 family 3	M	V309F/-	14	0.84 (±0.1)	4.05
Female Carriers					
II2 family 2	F	M115V/wt	46	7.52 (±1.62)	36.2
II4 family 2	F	M115V/wt	49	7.22 (±0.11)	34.7
II6 family 2	F	M115V/wt	60	9.93 (±0.46)	47.7
II2 family 3	F	V309F/wt	52	3.8 (±0.64)	18.3
Unaffected Male					
III1 family 2	M	wt/-	18	22.10 (±0.12)	106.2
Unrelated Controls					
CTR-1	M	wt/-	46	15.43 (±3.01)	74.2
CTR-2	F	wt/wt	44	17.02 (±4.26)	81.8
CTR-3	F	wt/wt	29	23.03 (±3.96)	110.7
CTR-4	M	wt/-	23	26.44 (±4.94)	127.1

Figure 3 Functional characterization of the identified *PRPS1* variants. (**a**) PRS-I activity in erythrocytes was evaluated by measuring the accumulation of AMP by HPLC in five affected males, four female carriers, as well as five healthy control individuals (wt). The diagram shows the correlation between ribose-5-phosphate-dependent AMP generation (y axis) and the reaction incubation time (x axis). Error bars represent the standard error of the mean (SEM) for genotypes represented by >1 individual (wt, $n=5$; M115V/-, $n=2$; M115V/wt, $n=3$; A113S/-, $n=2$), whereas they indicate the standard deviation (SD) for genotypes represented by a single individual. (**b**) Summary of the functional data obtained from PRPP synthetase activity assay. The enzyme activity is expressed as nmoles of AMP per milligram of Hb per hour. SD was calculated from three independent experiments performed in triplicate. The percentage was calculated as the ratio between the individual PRS-I activity and the mean of the PRS-I activity of the unaffected male and wt controls (range of PRS-I activity in controls: 15.43–26.44 nmol/mg/h).

patients II2 and II4 from Family 1 was 5.29 and 7.33 nmol/mg/h, respectively, whereas in the Family-2 III2 and III4 patients the enzyme activity was reduced to 2.11 and 1.06 nmol/mg/h and in the Family-3 proband to 0.84 (range of PRS-I activity in controls: 15.43–26.44 nmol/mg/h).

PRPS1 allelic expression is unbalanced in the female carrier of the p.(V309F) mutation

The female carriers of p.(M115V) and p.(V309F) have different hearing phenotypes, although they both showed a decreased PRS-I activity similar to that observed in patients hemizygous for the p.(A113S) substitution. Therefore, we investigated the possibility of an unbalanced expression of the wild-type (wt) and the mutant alleles, by comparing the sequence of *PRPS1* mRNA at the mutant position, amplified by RT-PCR from PBMC RNA, with that obtained from genomic DNA (Supplementary Methods). The results showed a preferential expression of the mutant *PRPS1* allele in the c.343A>G carrier of Family 2 (60 *vs* 40%) (Supplementary Figure 2A) and an almost-exclusive expression of the wild-type *PRPS1* allele in the c.925G>T carrier of Family 3 (85 *vs* 15%) (Supplementary Figure 2B). However, while the unbalanced allelic expression observed in the individual from Family 2 is not due to a skewed inactivation of the X-chromosome, as determined by methylation assays, in the II2 carrier from Family 3 a mild skewed inactivation ($\geq$75%) of the mutant X-chromosome is evident (Supplementary Methods and Supplementary Figure 2).

DISCUSSION

The high genetic heterogeneity of sensorineural HL makes the screening of all candidate genes by traditional methods unfeasible. In the present study, WES of a single proband allowed the molecular diagnosis of the genetic defect (c.337G>T (p.A113S)) underlying post-lingual hearing impairment in an X-linked NSHL family. The subsequent mutational screening of *PRPS1* by Sanger sequencing in 16 unrelated male probands with a likely X-linked deafness identified two additional missense variants, c.343A>G (p.M115V) and c.925G>T (p.V309F), segregating with early-onset HL. All three variants are novel and affect amino acids that are highly evolutionarily conserved, from zebrafish to humans (Supplementary Figure 3). More importantly, we show that molecular diagnosis could guide additional clinical evaluations to reveal subtle or subclinical neuropathy that might otherwise be overlooked. Indeed, two of the families carrying novel variants (Families 2 and 3) were initially diagnosed as having NSHL, but following the identification of missense substitutions in *PRPS1* they underwent neurological evaluation, and displayed signs and symptoms of peripheral neuropathy, at various severity (Supplementary Table 4). In this frame, our data significantly increase the mutational spectrum of *PRPS1*-associated NSHL/CMTX5 phenotypes, since only seven missense mutations, four responsible for NSHL (c.193G>A (p.D65N), c.259G>A (p.A87T), c.869T>C (p.I290T), and c.916G>A (p.G306R)), and three for CMTX5 (c.129A>C (p.E43D), c.344T>C (p.M115T), c.362C>G (p.A121G)), have been described so far.[6,11,12] We now report, and characterize by both *in-silico* structural analysis and *in-vitro* enzymatic assays, three novel mutations, thus contributing in better understanding the impact of different variants on the enzyme function, as well as genotype–phenotype correlations.

PRS-I is thought to be physiologically functional as a hexamer, which consists of three homodimers arranged in a propeller-like shape, each with an active site and two regulatory allosteric sites.[18] The active site comprises binding sites for both ATP and ribose-5-phosphate, is largely located at the interface of two subunits within one homodimer (dimer interface), and extends to the interface between homodimers (trimer interface). All previously reported NSHL-causing mutations are predicted to either disturb the local stability of PRS-I or moderately affect interactions at the trimer interface; conversely, CMTX5-causing mutations are likely to affect both the ATP-binding pocket and the allosteric site I.[8]

The p.(A113S) mutation is located in an alpha-helix participating to the trimer interface, and is predicted to destabilize the surrounding environment, possibly affecting ATP binding (Figures 4a and b). Met115 is located in the same alpha-helix, and is pointing toward the trimer interface; the M115V substitution is predicted to disturb the packing, likely destabilizing the ATP-binding site and the allosteric site I (Figures 4c and d). Finally, Val309 is part of the allosteric site I and is located at the trimer interface near the center of the hexamer. The introduction of a phenylalanine is predicted to disturb the allosteric site I function as well as the hexameric assembly (Figures 4e and f).

Summarizing, the here-reported missense variants are expected to exert a mild destabilization of the hexameric enzyme structure, although p.(M115V) and p.(V309F) are predicted to have a more severe effect than p.(A113S). Enzymatic assays, performed on erythrocytes of compliant patients and controls, substantially confirmed these *in-silico* predictions. All analyzed mutations resulted in a marked reduction (>60%) of PRS-I activity in the patients, p.(M115V) and p.(V309F) leading to a much more severe decrease (to ~6% of normal enzyme activity) than p.(A113S) (~30% residual activity). These results well correlate with clinical data, with p.(A113S) being responsible of the sole NSHL, and p.(M115V) and p.(V309F) resulting in the presence of peripheral neuropathy (Table 1). It is interesting to note that p.(M115V) involves the same residue that was found mutated (p.(M115T)) in a previously described CMTX5 kindred,[11] suggesting that Met115 might be particularly critical for enzyme function (Supplementary Figure 4).

Inter- and intra-familial phenotypic variability of disease expression has been reported for Arts syndrome, CMTX5, and PRS-I superactivity, sometimes with overlapping phenotypes even within individuals.[14,15] Here we show a wide, and almost continuous, spectrum of neurological manifestations in CMTX5, ranging from a subclinical peripheral neuropathy with prevalent axonal motor neuropathy (Family 3), to an axonal sensory-motor neuropathy (Family 2) (Supplementary Table 4). Attenuation/exacerbation of the clinical manifestations may be due to several biological factors, such as (i) functional redundancy and partial compensation by other PRS isoforms; (ii) differences in the expression levels of the rate-limiting enzyme, PRPP amidotransferase (PPAT); (iii) the presence of additional modifier *loci*; or, in females, (iv) skewed X-chromosome inactivation. Indeed, we observed a mild skewed inactivation of the mutant *PRPS1* allele in the c.925G>T (p.V309F) II2 carrier from Family 3, who has both normal audiologic and EMG parameters, whereas no skewed X-inactivation was detected in the c.343A>G (p.M115V) heterozygous female (II2, Family 2), who is mildly deaf and shows chronic denervation at EMG (Supplementary Figure 2). We also attempted to verify whether the expression levels of genes involved in the purine metabolism pathway (eg, *PRPS2, PPAT,* and *HGPRT*) could contribute to the phenotypic variability among the three analyzed families by a compensatory-based mechanism. We observed increased expression only for the *HGPRT* transcript in heterozygous female carriers in comparison with healthy controls (almost 2-fold increase, $P=0.01$; Supplementary Figure 5). These data should however be considered with caution, since *HGPRT* itself is an X-linked gene and the number of available heterozygous

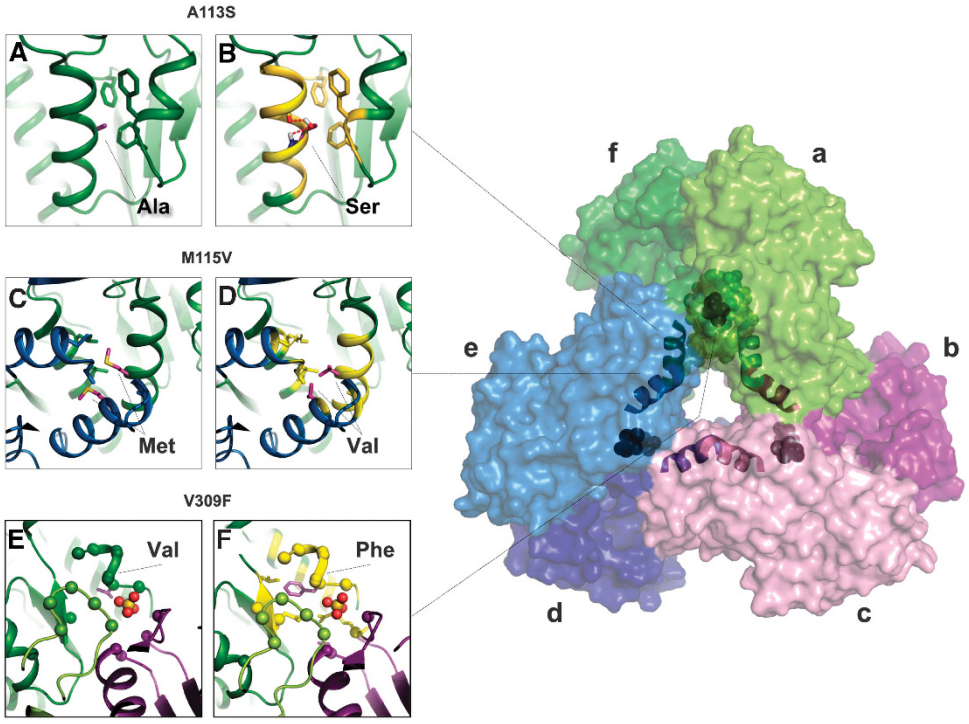

Figure 4 Structural analysis of the newly identified PRS-I missense variants. On the right: Molecular surface of the three-dimensional structure of the PRS-I enzyme in its physiologic assembly, with the six different subunits (a to f) indicated by separated colors. The two monomers forming a dimer are highlighted with different shades of the same color. The alpha-helices hosting A113S and M115V substitutions are shown as ribbons. Residue Val309 is shown by spheres. The allosteric sites of subunit a (dark green) are highlighted with a darker surface. The mutated residues discussed in the panels are from subunit a. The predicted ddG of the hexamer structure is 9.88, 15.57, and 26.53 kcal/mol in the presence of A113S, M115V, and V309F, respectively. (**A**, **B**) Structural analysis of the c.337G>T (p.A113S) variant. Left: Ala113 is completely buried in the hydrophobic core of the corresponding subunit, interacting with Phe92 (belonging to the flexible loop), Phe137, and Phe138. Right: Ser113 differs from Alanine in that one of the methylenic hydrogens is replaced by a hydroxyl group, through which this amino acid makes a new hydrogen bond. The larger and polar (hydrophilic) side chain of Ser113 makes this region to rearrange (highlight in yellow). (**C**, **D**) Structural analysis of the c.343A>G (p.M115V) variant. Left: Met115 is completely buried at the trimer interface, making hydrophobic interactions with the surrounding amino acids. Two Methionine 115 side chains from two different PRS-I dimers participate in a hydrophobic interaction at the interface. Right: Val115 is a beta-branched residue, introducing a completely different steric hindrance, making this region to rearrange (highlight in yellow). (**E**, **F**) Structural analysis of the c.925G>T (p.V309F) variant. Left: Val309 is part of the allosteric site I and is located at the trimer interface near the center of the hexamer. Right: Phe309 is bulkier than Val and surrounding residues are predicted to move to avoid Van der Waals crashes. Residues of allosteric site I are indicated with spheres. A sulphate ion present in the crystal structure is also shown that occupies the position of the b-phosphate of ADP; indeed an activator phosphate and an inhibitor ADP compete for binding at the allosteric regulatory site. In all panels, the mutated residue is shown by sticks: C atoms are colored magenta, O red, S yellow, and H white. Residues predicted by FoldX to be perturbed are colored in yellow.

Table 1 Summary of genetics and clinical features of patients carrying newly identified *PRPS1* mutations

			Hemizygous male patients				
Nucleotide change[a]	*AA change*[b]	*Functional change*	*Hearing status*	*Severity*	*Progression*	*Hearing status in female carriers*	*Neurological symptoms*
c.337G>T	p.A113S	Loss of function	HL onset in first decade, affecting all tones	Profound	Yes	Moderate HL	No
c.343A>G	p.M115V	Loss of function	HL onset in first decade, affecting all tones	Moderate to profound	Yes	Mild to moderate HL	Yes
c.925G>T	p.V309P	Loss of function	HL onset in first decade, affecting all tones	Moderate to profound	Yes	Normal	Yes

[a]Numbering refers to NM_002764.3 mRNA sequence.
[b]Numbering refers to NP_002755.1 protein sequence.

female carriers is not sufficient to reach a robust statistical significance.

Finally, the description and characterization of novel *PRPS1* mutations has important consequences not only for diagnosis, but also for therapeutic and prevention purposes. Indeed, despite the central role of PRS-I enzyme in *de-novo* purine synthesis, purine nucleotides can be produced also by an alternative pathway, which uses S-adenosylmethionine (SAM).[8] Importantly, SAM appears to be able to cross the intestinal wall, the blood–brain barrier, and possibly the blood–labyrinth barrier, and has already been used as treatment for many different pathologies, including Arts syndrome.[15,24] Dietary supplementation with SAM in Arts syndrome patients, in particular,

alleviated their symptoms and stabilized the progression of hearing impairment.[8] Hence, SAM supplementation in the diet might represent a promising therapy to postpone/slow down the onset and progression of neurological and audiologic symptoms in patients with *PRPS1* mutations as well as in mildly affected female carriers.

CONFLICT OF INTEREST

The authors declare no conflict of interest.

ACKNOWLEDGEMENTS

This work has been supported by the Italian Telethon Foundation, grant numbers GGP11177 (to SD, RA, GS, UA, PC, and PP), GGP12024 and GGP10007 (to SCP), as well as Fondazione Cariplo, grant no 2013-0825 (to RA). We are indebted to the study subjects for their participation, without which this research would be impossible. Nicole Tonsi and Stefano Lancillotti are also acknowledged for their invaluable assistance and technical support.

1 Raviv D, Dror AA, Avraham KB: Hearing loss: a common disorder caused by many rare alleles. *Ann NY Acad Sci* 2010; **1214**: 168–179.
2 Walsh T, Shahin H, Elkan-Miller T *et al*: Whole exome sequencing and homozygosity mapping identify mutation in the cell polarity protein GPSM2 as the cause of nonsyndromic hearing loss DFNB82. *Am J Hum Genet* 2010; **87**: 90–94.
3 Schraders M, Haas SA, Weegerink NJ *et al*: Next-generation sequencing identifies mutations of SMPX, which encodes the small muscle protein, X-linked, as a cause of progressive hearing impairment. *Am J Hum Genet* 2011; **88**: 628–634.
4 Huebner AK, Gandia M, Frommolt P *et al*: Nonsense mutations in SMPX, encoding a protein responsive to physical force, result in X-chromosomal hearing loss. *Am J Hum Genet* 2011; **88**: 621–627.
5 de Kok YJ, van der Maarel SM, Bitner-Glindzicz M *et al*: Association between X-linked mixed deafness and mutations in the POU domain gene POU3F4. *Science* 1995; **267**: 685–688.
6 Liu X, Han D, Li J *et al*: Loss-of-function mutations in the PRPS1 gene cause a type of nonsyndromic X-linked sensorineural deafness, DFN2. *Am J Hum Genet* 2010; **86**: 65–71.
7 Becker MA: Phosphoribosylpyrophosphate synthetase and the regulation of phosphoribosylpyrophosphate production in human cells. *Prog Nucleic Acid Res Mol Biol* 2001; **69**: 115–148.
8 de Brouwer AP, van Bokhoven H, Nabuurs SB, Arts WF, Christodoulou J, Duley J: PRPS1 mutations: four distinct syndromes and potential treatment. *Am J Hum Genet* 2010; **86**: 506–518.
9 Sperling O, Eilam G, Sara-Persky-Brosh, De Vries A: Accelerated erythrocyte 5-phosphoribosyl-1-pyrophosphate synthesis. A familial abnormality associated with excessive uric acid production and gout. *Biochem Med* 1972; **6**: 310–316.
10 Moran R, Kuilenburg AB, Duley J *et al*: Phosphoribosylpyrophosphate synthetase superactivity and recurrent infections is caused by a p.Val142Leu mutation in PRS-I. *Am J Med Genet* 2012; **158A**: 455–460.
11 Kim HJ, Sohn KM, Shy ME *et al*: Mutations in PRPS1, which encodes the phosphoribosyl pyrophosphate synthetase enzyme critical for nucleotide biosynthesis, cause hereditary peripheral neuropathy with hearing loss and optic neuropathy (cmtx5). *Am J Hum Genet* 2007; **81**: 552–558.
12 Park J, Hyun YS, Kim YJ *et al*: Exome sequencing reveals a novel PRPS1 mutation in a family with CMTX5 without optic atrophy. *J Clin Neurol* 2013; **9**: 283–288.
13 de Brouwer AP, Williams KL, Duley JA *et al*: Arts syndrome is caused by loss-of-function mutations in PRPS1. *Am J Hum Genet* 2007; **81**: 507–518.
14 Synofzik M, Müller Vom Hagen J, Haack TB *et al*: X-linked Charcot-Marie-Tooth disease, Arts syndrome, and prelingual non-syndromic deafness form a disease continuum: evidence from a family with a novel PRPS1 mutation. *Orphanet J Rare Dis* 2014; **9**: 24.
15 Liu XZ, Xie D, Yuan HJ, de Brouwer AP, Christodoulou J, Yan D: Hearing loss and PRPS1 mutations: Wide spectrum of phenotypes and potential therapy. *Int J Audiol* 2013; **52**: 23–28.
16 Primignani P, Trotta L, Castorina P *et al*: Analysis of the GJB2 and GJB6 genes in Italian patients with nonsyndromic hearing loss: frequencies, novel mutations, genotypes, and degree of hearing loss. *Genet Test Mol Biomarkers* 2009; **13**: 209–217.
17 Li R, Yu C, Li Y *et al*: SOAP2: an improved ultrafast tool for short read alignment. *Bioinformatics* 2009; **25**: 1966–1967.
18 Li S, Lu Y, Peng B, Ding J: Crystal structure of human phosphoribosylpyrophosphate synthetase 1 reveals a novel allosteric site. *Biochem J* 2007; **401**: 39–47.
19 Schymkowitz J, Borg J, Stricher F, Nys R, Rousseau F, Serrano L: The FoldX web server: an online force field. *Nucleic Acids Res* 2005; **33**: W382–W388.
20 Guerois R, Nielsen JE, Serrano L: Predicting changes in the stability of proteins and protein complexes: a study of more than 1000 mutations. *J Mol Biol* 2002; **320**: 369–387.
21 Krieger E, Koraimann G, Vriend G: Increasing the precision of comparative models with YASARA NOVA–a self-parameterizing force field. *Proteins* 2002; **47**: 393–402.
22 Torres RJ, Mateos FA, Puig JG, Becker MA: A simplified method for the determination of phosphoribosylpyrophosphate synthetase activity in hemolysates. *Clin Chim Acta* 1994; **224**: 55–63.
23 Balasubramaniam P, Malathi A: Comparative study of hemoglobin estimated by Drabkin's and Sahli's methods. *J Postgrad Med* 1992; **38**: 8–9.
24 Bottiglieri T: S-Adenosyl-L-methionine (SAMe): from the bench to the bedside–molecular basis of a pleiotrophic molecule. *Am J Clin Nutr* 2002; **76**: 1151S–1157S.

Supplementary Information accompanies this paper on European Journal of Human Genetics website (http://www.nature.com/ejhg)